Seismic wave scattering in volcanoes

Edoardo Del Pezzo

INGV - Osservatorio Vesuviano. Via Diocleziano, 328. 80124 Napoli

January 21, 2008

Abstract

Volcano-tectonic (VT) earthquakes produce high-frequency seismograms characterized by impulsive shear mechanism; their seismogram coda reflects the random inhomogeneity of the volcano structure. Consequently, this inhomogeneity can be investigated through the analysis of the coda wave envelopes of the VT events. In this chapter, I will review the main observational results obtained from volcanoes around the World, with the aim of quantifying the scattering and attenuation properties of the volcanic areas. First, I will review the coda-Q observations and their frequency dependence, then I will report on attempts that have been made to separate the intrinsic from the scattering attenuation using multiple scattering and diffusion models, and finally, I will report on the interpretations based on these results. The results show that the coda-Q absolute values characteristic of volcanoes are slightly smaller than those measured in non-volcanic zones, and that sometimes their frequency dependence is different. It is impossible to deduce by coda-Q observations only whether this difference is controlled more by the intrinsic or the scattering attenuation. The application of multiple scattering models allows separate estimates of the intrinsic and the scattering attenuation coefficients. Results show that volcanoes are highly heterogeneous structures, with a mechanism of seismic wave energy dissipation that tends to be controlled by the scattering phenomena with increasing frequency. For Mt. Vesuvius, Mt. Merapi and Deception island volcano scattering attenuation prevails at frequencies higher than 2-3 Hz. At Mt. Etna, intrinsic dissipation prevails or is comparable with scattering attenuation for frequencies lower than 8 Hz.

At high frequencies, diffusion approximation is appropriate to describe the energy seismogram envelope. The intrinsic dissipation of shear waves [possibly connected with magma reservoirs, which should decrease the intrinsic Q values for shear waves] only has an important role at low frequencies.

Key words: Seismic scattering, coda waves, volcanoes

INTRODUCTION

Volcanic earthquakes

Volcanoes are sites of peculiar seismic activity, which is generally classified into four categories: volcano-tectonic [VT] earthquakes, long period [LP] events, very long period [VLP] events and volcanic tremor (Chouet, 2003) . In typical observatory practice, this classification is carried out visually, by analyzing the seismogram shapes and/or the spectral contents of the waveforms. Modern research in volcano seismology, aimed at the quantification of the seismic phenomena associated with volcanc eruptions, enlighten the role played by magmatic and hydrothermal fluids in the generation of the seismic waves, making critically important the quantification of the source properties of LP and tremor. As the different events reflect different kinds of source mechanisms, the quantification of their source is crucial to determine the extent and evolution of the magmatic energy. In particular, LP events and tremor generally precede and accompany the eruptive phenomena [Chouet (2003) and references therein], and are used to assess the eruptive state or to estimate the eruptive potential. This is an obvious reason why monitoring the insurgence of this kind of seismicity is considered to be the most reliable and powerful techniques of volcano monitoring. One of the problems is that the seismogram shape of the volcanic quakes or, similarly, their spectral shape [frequency domain], is greatly dependent on the propagation effects, and hence on the elastic properties of the seismic medium. Consequently, the medium properties need to be studied carefully to correctly adjust for the effects of propagation and to obtain valid event classifications aimed at an understanding of the physics of a volcanic source.

VT events are located inside the volcano structure, generally at shallow depths [down to 10 km]. They are the brittle responses of the volcano materials to the magma processes and/or to changes in the thermal state of the rocks [the heating or cooling in the vicinity of a magma body]. VT may also reflect far-field stresses acting on heterogeneous materials and changes in the pore pressure. The impulsive shear mechanism of these events produces high-frequency seismograms that reflect the random heterogeneity of the volcano structure in their coda. The heterogeneity of volcanoes can thus be investigated through the analysis of the VT coda wave envelopes. Other volcanic earthquakes, on the contrary, are characterized by non-impulsive and time-persistent sources, which generate complex coda waveforms. In this case, the problem of separating the radiation generated by the scattering phenomena from that related to the source is more difficult.

Due to the impulsive shear mechanism that generates the high frequency content of the coda, VT earthquakes are the most suitable for investigations into small-scale heterogeneity characterizing the earth medium beneath volcanoes.

A brief review of coda-Q^{-1} observation on volcanoes

The first attempts to quantify the scattering and attenuation parameters for rocks constituting the volcanic structures, were carried out using the estimate of coda-Q^{-1}, or Q_C^{-1} of the local VT earthquakes. As is well known, this parameter describes the the energy density decay of the short period seismogram, $E^{SS}(\mathbf{x}, t)$, recorded at position $\mathbf{x}$ and at the time t due to an impulsive source applied at $\mathbf{x}_0$ in the single scattering assumption [Sato and Fehler (1998) section 3.1.2] as

$$E^{SS}(\mathbf{x}, t) = \frac{E_0 g_0}{4\pi \left|\mathbf{x} - \mathbf{x}_0\right|^2} K \left(\frac{\beta t}{|\mathbf{x} - \mathbf{x}_0|} \right) H \left(\beta t - |\mathbf{x} - \mathbf{x}_0| \right) e^{-\omega t Q_C^{-1}} \tag{1}$$

whereE_0 is the energy density at the source, g_0 is the scattering coefficient, β is the seismic velocity for the shear waves (taken as a constant), H is the Heaviside step function, K is a term depending on geometrical spreading and distance and ω is the angular frequency. With short hypocentral distances [source is assumed to be co-located with the receiver] formula 1 can be approximated by

$$E^{SS}(t) \simeq \frac{E_0 g_0}{2\pi \beta^2 t^2} e^{-\omega t Q_C^{-1}} \tag{2}$$

Using these assumptions [often respected by VT earthquakes, that are generally recorded by stations close to the source], Q_C^{-1} appears to include both absorption and scattering losses [see Sato and Fehler (1998), sections. 3.1., 3.3.2 and 7.1.1] although its physical meaning has been controversial for many years. The idea that coda-Q^{-1} accounts for both intrinsic and scattering attenuation prevailed untill the appearance in the literature of theoretical (Shang and Gao, 1988), numerical (Frankel and Clayton, 1986) and laboratory (Matsunami, 1991) studies concluding that coda-Q^{-1} is essentially an estimate of intrinsic-Q^{-1}. More recently, Zeng (1991) described the solution of the integral equation for the seismic energy density, $E(\mathbf{x}, t)$, recorded at position $\mathbf{x}$ and at the time t due to an impulsive source applied at $\mathbf{x}_0$. The integral equation, that is equivalent to the equation of radiative transfer in case of isotropic scattering, is given by

$$E(\mathbf{x}, t) = E_0 \left(t - \frac{|\mathbf{x} - \mathbf{x}_0|}{\beta} \right) \frac{e^{-\eta|\mathbf{x}-\mathbf{x}_0|}}{4\pi \left|\mathbf{x} - \mathbf{x}_0\right|^2} + \int_V \eta_S E \left(\xi, t - \frac{|\mathbf{x} - \boldsymbol{\xi}|}{\beta} \right) \frac{e^{-\eta|x-\xi|}}{4\pi \left|\mathbf{x} - \boldsymbol{\xi}\right|^2} dV(\boldsymbol{\xi}) \tag{3}$$

where $E_0 \left(t - \frac{|\mathbf{x}-\mathbf{x}_0|}{\beta} \right)$ represent the impulsive Energy radiated by the source, $\eta = \eta_S + \eta_I$ is the total attenuation coefficient, with η_S and η_I respectively the scattering and the intrinsic attenuation coefficients, and ξ is the variable of integration (describing the spatial position of the scatterers). The quality factors for scattering and intrinsic attenuation can be expressed in terms of attenuation coefficients by

$$Q_{S,I}^{-1} = \eta_{S,I}\beta/\omega \tag{4}$$

where subscripts S and I stand for scattering and intrinsic, respectively. The assumptions underlying equation (3) are more general than those for the equation (1), as all multiple scatterings are included. In both equations (1) and (3) scattering is assumed to be isotropic and the medium randomly uniform.

Formulas (1) and (2) have been widely used for fitting the experimental coda envelopes to invert for Q_C^{-1}. Results obtained over time and throughout the World have been used to characterize the average attenuation properties of the zones under study simply by comparing coda-Q^{-1} parameters. Unfortunately, as reported above, the physical interpretation may be confusing. Moreover, there is an additional problem of interpretation of these early results, due to their significant dependence on the time window in which the fit of data with single scattering model is made. This dependence is often named "lapse time dependence of Q_C". Due to this dependence [Q_C^{-1} decreases with lapse time], the experimental results reported without an explicit specification of the lapse time window length used for calculations may be not strictly suitable for comparison among the different areas. Figure 1 shows a compilation of Q_C^{-1} observations made in volcanic areas using similar lapse time window lengths (or I explicitly report the lapse time used). Looking at the plots of Figure 1 it can be noticed that in some cases coda-Q pattern show a peculiar frequency pattern. This is particularly evident for Kilauea, Mt. S. Helens and Mt. Vesuvius. A comparison with Q_C^{-1} estimates in stable or tectonically active non-volcanic areas using data taken from Ibanez (1990) and Del Pezzo et al (1996), is reported in Figure 2 for the volcanic area of Mt. Etna (Italy) and the non-volcanic zone of Andalucia (Spain). The plots reproduce estimates obtained at the same lapse time intervals. Leaving aside the interpretation of the physical meaning, these plots show that Etna volcano behaves differently from the tectonically active sedimentary Granada basin, showing an overall higher coda-wave attenuation.

The results reported in Figure 1 show that in some cases [Etna, Kilauea and Vesuvius] there is a frequency dependence that is weaker than or opposite (Q^{-1} increasing with frequency) to the other regions. Whether these differences are controlled more by intrinsic or by scattering attenuation is impossible to deduce by examining only Q_C^{-1} observations. A further difficulty in the interpretation of Q_C^{-1} is given by the uniform half space assumption. Gusev (1995) found that Q_C^{-1} may be closer to the real Q_I^{-1} for earth media characterized by strong velocity gradients. This study demonstrated that coda decay is quantitatively well explained if the scattering coefficient decreases with depth, when the leakage of scattered energy to the bottom cannot be discriminated from intrinsic loss. Margerin et al (1998) and Wegler (2004) using the diffusion approximation derived analytical expressions which describe the coda decay due to leakage, in the assumption of a heterogeneous layer superimposed to a transparent half space.

It can be concluded that there is no simple relation between Q_C^{-1} and scattering and intrinsic inverse-Q. Consequently, separate estimates of intrinsic and scattering attenuation coefficients performed by using the realistic assumptions of positive (with depth) seismic velocity gradients and depth-dependent attenuation parameters are necessary to quantify the scattering processes in volcanic regions.

SEPARATED ESTIMATES OF INTRINSIC AND SCATTERING ATTENUATION

To date, the most complete approach to characterize the earth medium for optimally describing energy propagation and scattering properties has been the radiative transfer theory, which includes multiple scattering of any order (Ryzhik et al, 1996). This theory allows the analytical description of the coda envelope as a function of source-receiver distance and lapse time, in the hypothesis of a uniform medium and isotropic scattering (Zeng, 1991) . Numerical simulation is needed to describe more realistic media, characterized by non-isotropic scattering and/or non-uniform velocity and scatterer distributions [Hoshiba et al (1991), Gusev and Abubakirov (1996)]. This theory can be fitted to the experimental coda envelope to directly invert the scattering and dissipation attenuation coefficients, and is well suited to model the seismic coda on volcanoes.

This inversion for attenuation coefficients has often been carried out with the multiple lapse-time window analysis [MLTWA] technique, as described by Hoshiba (1993). This analysis is based on calculation of the seismogram energy integrals across three successive time windows, as a function of the source-receiver distance and medium parameters. The three energy-distance curves are then fitted to the theoretically determined values, to retrieve the scattering attenuation and the intrinsic dissipation coefficients [for a detailed discussion of this method, see also Sato and Fehler (1998), pages 190-191]. Due to the low velocity of the S-waves in the shallowest layers of the volcanic areas [as low as 1.5 km/s], to the short duration of the seismograms of VT earthquakes, and to the limited intervals of source-station distance generally available for these kinds of earthquakes, the integrals in the three successive time windows cannot generally be calculated with sufficient numbers of data points, and the distance range is insufficient to make the fit stable. Consequently, the application of MLTWA to volcanoes may become difficult. For this reason, previous attempts carried out to separately estimate intrinsic and scattering attenuation coefficients for local volcanic earthquakes are based on different and sometimes approximate techniques. In the following sections, I will review the approaches used to experimentally study the scattering properties of volcanic areas and I will discuss the results obtained.

The method of Wennerberg

One of the first attempts to separately obtain scattering and intrinsic attenuation parameters in volcanic areas was done for the zones of Etna and Campi Flegrei [Italy] (Del Pezzo et al, 1995) using an approach developed by Wennerberg (1993). This study suggested the possibility of reinterpreting the estimates of single-station Q_C^{-1} values in terms of multiple scattering. It used the approximation given by Abubakirov and Gusev (1990) to the Energy transport theory in the formulation of Zeng (1991) to describe the multiple-scattered wave field in the case of a source co-located with the station. Wennerberg (1993) expresses Q_C^{-1} as a function of Q_I^{-1} and Q_S^{-1} as:

$$Q_C^{-1} = Q_I^{-1} + [1 - 2\delta(\tau)]Q_S^{-1} \tag{5}$$

where $\delta(\tau) = \frac{-1}{4.44+0.738\tau}$ and $\tau = 2\pi f t Q_S^{-1}$. Using the definition of $Q_T^{-1} = Q_I^{-1} + Q_S^{-1}$, the total inverse quality factor for S-waves, this method allows the estimation of Q_I^{-1} and Q_S^{-1} from (independent) measurements of Q_T^{-1}, and Q_C^{-1} . The method is strictly applicable to local earthquake data recorded at stations close to the source for which the direct ray-paths share the same volume encompassed by the scattered waves. Results obtained for Etna volcano and Campi Flegrei areas were compared with the tectonically active non-volcanic zone of Granada Basin, for which the same experimental conditions were encountered [shallow sources located close to the recording stations - 20 s maximum lapse time for Q_C^{-1}]. The results for Q_C, Q_T, Q_I and Q_S are summarized in Table 1 of Del Pezzo et al (1995). Martinez Arevalo et al (2003) applied the same method to local VT earthquakes recorded at a small aperture (300 m) array composed of 13 short period sensors, located in Deception Island, Antarctica. Deception is the most important active volcano of the South Shetland Islands, and is located northeast of the Antarctic Peninsula. Results are reported in Fig. 17 of Martinez Arevalo et al (2003).

The plot of Figure 3 show the results obtained for Etna and Deception [those for Campi Flegrei after being reviewed by Del Pezzo et al (1996) were shown to be based on a rough estimate of total Q-inverse, and will be discussed later]. For the sake of uniformity with the plots of the present study, I have plotted Q-inverse (instead of Q) with its error bars for Etna and Deception Island, and compared the results obtained with those of the tectonically active area of Andalucia. The plot shows that the earth lithosphere beneath volcanoes (Etna and Deception) and the tectonically active area of Andalucia (Granada basin) have different scattering properties: the two volcanic zones are more heterogeneous than the tectonically active zone of the Granada basin. Attenuation at Etna is controlled by intrinsic dissipation at frequencies below 8 Hz, whereas for the higher frequency bands, dissipation and scattering effects are comparable. At Deception only the frequency bands higher than 7 Hz are available. For high frequencies, scattering effects predominate over the intrinsic dissipation at Deception.

The Energy flux model

An approximate method, different from that described in the previous section, for obtaining separate estimates of intrinsic and scattering attenuation parameters was applied to Campi Flegrei area, close to Naples, Italy, by Del Pezzo et al (1996). These study used the energy-flux model for coda generation in a uniform medium (Frankel and Wennerberg, 1987) - see formula 3.34 of Sato and Fehler (1998) . The energy-flux model is a phenomenological model based on the assumption that coda envelopes, recorded at different distances, approach the same value for increasing lapse time. In contrast to that of Wennerberg (1993), this method, inverts the coda envelope and does not use an independent estimate of Q_T^{-1}.The results are obtained assuming a-priori a frequency dependence of Q_S^{-1}. Del Pezzo et al (1996) assume that $Q_S^{-1} = q_0 f^{-n}$ and calculate both Q_S^{-1} and $Q_I^{-1}$for a suite of n values, spanning the interval between 0.1 and 0.9. Here I report in Table **??** only those for $n = 0.9$ and for $n = 0.1$, corresponding to a strong frequency dependence and an almost constant Q_S^{-1} with frequency, respectively. Results were obtained for three frequency bands (centered at 6, 8 and 10 Hz, respectively).

At Etna, as also in the area of Campi Flegrei, scattering phenomena strongly predominate over inelastic dissipation.

2-D transport theory applied to Volcanic tremor

Volcanic tremor is a sustained seismic signal which is often seen in association with magmatic activity. Its importance as a forecasting tool of eruptions has been widely acknowledged since many years [e.g. Chouet (2003), and references therein]. The mechanism of the tremor source is still under debate, although the generation of the sustained ground motion is generally ascribed to the trapping of elastic energy in fluid-filled cavities. Studying the tremor sources is, however, challenging, due to the main reason that tremor signal is quasi-stationary, with no clear onsets and/or clear phases that can be ascribed deterministically to a particular path. Moreover, the signal generally looses coherency with increasing station spacing, making it impossible to adopt classical tools for locating sources and separating path, source and site effects. An understanding of the scattering properties of the volcanic media for the tremor wave propagation is consequently an important task that should be properly addressed.

The first measurements of the total attenuation for tremor waves were carried out by Del Pezzo et al (1989) at Etna volcano, who simply calculated the spectral amplitude decay of the tremor as a function of source-station distance. The results show that total Q-inverse is frequency dependent with data fitting well the relation $Q_T^{-1} = q_0(\frac{f}{f_0})^{-n}$ with $f_0 = 1\ Hz$, $n = 0.7$ and $q_0 = \frac{1}{12}$. Lower values of Q_C^{-1} and Q_T^{-1} calculated for VT-earthquakes in the same area [see the previous section of the present chapter] were interpreted in terms of a strong depth dependence of attenuation: as the tremor wave propagation is essentially shallow [the tremor is mainly composed of a mixture of surface waves], it samples the highest attenuation layers. A first attempt to separately estimate intrinsic and scattering attenuation coefficients for volcanic tremor has been carried out by Del Pezzo et al (2001) utilizing data recorded at Etna by Del Pezzo et al (1989) and at Masaya volcano by Metaxian et al (1997). The method is based on the energy transport theory in two dimensions (Sato, 1993). The space and time pattern of the tremor seismic energy is calculated by convolution of the source function with the energy density for an impulsive source radiation. The source time function for tremor is assumed to be constant, in the hypothesis of time- and frequency-stationary emission of seismic energy, and the convolution integral reduces to the following expression

$$\begin{aligned} E_{Tremor}(r) \quad \sim \quad & \int_{-\infty}^{+\infty} E(r,t)dt = \frac{\frac{1}{2\pi r}\exp\left[-(\eta_S + \frac{\eta_I}{v(f)})r\right]}{|v(f)|} + \\ & + \int_{r/v(f)}^{+\infty} \frac{\eta_S}{2\pi\sqrt{v(f)^2t^2 - r^2}} \exp\left[\eta_S\sqrt{v(f)^2t^2-r^2} - v(f)t\right] \exp(-\eta_I t)dt \end{aligned} \tag{6}$$

where $E_{Tremor}(r)$ is the tremor energy as a function of distance, r, the frequency, f, the wave speed, $v(f)$, the intrinsic attenuation coefficient, η_I, the scattering attenuation coefficient, η_S, and the lapse time, t. $v(f)$ represents the wave velocity in a dispersive wave field. $E(r,t)$ is the Green's function for an impulsive source [Sato and Fehler (1998) pages 173-176].

Formula (6) was fit to the experimentally measured tremor energy decay with distance. The best estimates of η_I and η_S were obtained with a grid search method, and the results for Q_S^{-1} and Q_I^{-1} derived from formula (4) are given in Table 2. Despite the trade off between the estimate of Q_I^{-1} and Q_S^{-1}, the results show that the mechanism of dissipation is predominant over scattering phenomena in the characterization of the seismic attenuation of tremor for both volcanoes under study. This is in contrast to the earlier results for VT events at Campi Flegrei, Etna and Deception. This contradictory result may have a geological explanation, as the uppermost layers composing the structure of Etna are spatially homogeneous (smaller amount of scattered energy) , all composed by loose and incoherent materials (high intrinsic dissipation).

DIFFUSION MODEL APPLIED TO SHOT DATA

Uniform half-space

Hereafter I will focus attention on two volcanoes, Vesuvius and Merapi, where most of the studies dealing with the application of the diffusion model [that will be described in the present and in the following sections], have been done.

The transport theory has an important asymptotic approximation in the case of strong scattering: the diffusion theory (Wegler, 2004). This approximation is mathematically much simpler and can be analytically expressed in case of a medium composed of two layers with different characteristics. The analytical expression for an homogeneous earth medium is

$$E(|\mathbf{x}|, t) = E_0 (4\pi D t)^{-p/2} e^{(-bt - \frac{|\mathbf{x}|^2}{4Dt})} \tag{7}$$

where $p = 3$ for body waves and $p = 2$ for surface waves. $p = \beta / \eta_S D$ and $b = \eta_I \beta$. D is named "diffusivity".

The presence of diffusive waves was revealed experimentally in the seismograms of artificial shots fired at Merapi [Indonesia; Wegler and Luhr (2001)] and at Vesuvius (Wegler, 2003) during active tomography experiments. In these two cases, a rapid decrease of direct S-wave energy was observed and detected up to a distance of less than 1 km from the source. Despite this rapid decrease, the coda of the seismogram shots exhibits increasing amplitudes up to a lapse time much greater than the S-wave travel time and a slowly decaying amplitude for longer lapse time. Observations at small aperture arrays set up at Merapi (Wegler and Luhr, 2001) and at Mt. Vesuvius (La Rocca et al, 2001) in the time period of the active experiments showed that the coherence among the array stations is lost at distances smaller than a few tens of meters for frequencies higher than 1 Hz; the polarization properties calculated at the array stations also show that the pattern is chaotic, being the three components of the ground motion almost uncorrelated. This evidence is phenomenologically interpreted by Wegler and Luhr (2001) as the product of a diffusive wave field composing the coda of the seismogram shots.

Fitting the experimentally calculated energy envelopes to the expression of formula (7) it is possible to invert for D and b and to separately obtain the intrinsic and scattering attenuation coefficients.

The pattern of intrinsic and scattering attenuation as a function of frequency [averaged over distance] for Mt. Vesuvius and for Merapi obtained for the shot data is reported in Figure 4. In both cases, scattering predominates over inelastic dissipationby at least one order of magnitude in the analyzed frequency range. Wegler and Luhr (2001) estimate that the transport mean free path η_S^{-1} is of the order of 100 m for Merapi whereas Wegler (2003) estimate $\eta_S^{-1} = 200\ m$ for Mt. Vesuvius [for a wide and exhaustive discussion about the physical meaning of the transport mean free path, see Gusev and Abubakirov (1996)]. In both studies, a dominance of S-waves in the coda of the seismogram shots is assumed. This estimate is consistent with the assumption that diffusion is a valid approximation when source-station distance is much greater than the transport mean free path. In their experiments, source-station distance is always greater than 1 km. Almost the same diffusivity value is obtained assuming a three- or a two-dimensional propagation. This is due to the strong influence of the term $e^{(-bt-\frac{x^2}{4Dt})}$ in formula (7) with respect to the term accounting for geometrical spreading.

The above results indicate that multiple scattering cannot be neglected in the modeling of seismic wave propagation and in studying seismogram formation in volcanic areas. The comparison of the transport mean free path at Vesuvius and Merapi ($\simeq$ 200 m) with the much higher value estimated for the earth's crust ($\simeq$ 200 km) leads to the important conclusion that the multiple scattering strongly affects the seismogram shape for sources close to or within volcanoes. An indirect confirm of this important observation comes from high resolution velocity tomography carried out in volcanoes [see e.g. Scarpa et al (2002) , Chouet (2003) and references therein] which shows high velocity contrasts in small scale structures. This result cannot be neglected in any modeling of seismic wave propagation in volcanic environments.

Two layer media

The uniform random medium assumes that heterogeneity is uniformly distributed in the propagation volume. On the other hand, it is quite reasonable and well accepted that the earth properties change with increasing depth. The transport equation (3) can be solved analytically for a uniform random medium with a uniform scatterer distribution. Numerical simulation is necessary in the case of non-uniform velocity and/or scatterer density [see e.g. Hoshiba et al (2001)]. In the approximation of strong scattering, the diffusion equation can be solved for a two-layer model formed by a shallower diffusive layer over a weakly scattering half space. Margerin et al (1998) proposed a boundary condition for the layer half space including deterministic reflections. Wegler (2005) presents an improved boundary condition for the diffusion equation connecting a strongly scattering layer to a weakly scattering half space. This condition has a wide range of validity, failing only when the the thickness of the upper layer (the strong scattering layer) is smaller than its transport mean free path, and/or when a large contrast in scattering strength between the upper layer and the half space exists. The application of this two-layer model to volcanoes is straightforward, as volcanoes are highly heterogeneous structures in their upper part, due to the presence of lava and ash formations; and generally less heterogeneous in their deeper portion, made up by the last part of the upper crust. An understanding of the diffusive characteristics of the volcanic media using this realistic earth model may explain why the scattering strength apparently decreases with the increasing source-receiver distance when it is estimated assuming a half space model.

This approach has been used to study Merapi (Wegler, 2005) and Mt. Vesuvius (Wegler, 2004). At Merapi, the application of the theory to the same data set used by Wegler and Luhr (2001) yields new insight in the seismogram interpretation. For shot data [where the source is located at the surface] the coda envelopes well fit to a model with a diffusivity coefficient in the upper layer equal to 0.027 $km^2 s^{-1}$ [corresponding to $Q_S^{-1} = 0.7$ at 6 Hz] and in the lower half space equal to 0.3 $km^2 s^{-1}$ [corresponding to a $Q_S^{-1} = 0.06$]. The data inversion yields the position of the half space boundary at 0.5 km depth below the zero level. This model explains well the differences in the estimates of diffusivity obtained at different source-station distances for the uniform half-space model, fitting the data well at both short and long distance [see Fig. 5 of Wegler, 2005]. For Mt. Vesuvius, Wegler (2004) uses the same data set utilized in the work done assuming a half space [see also Fig. 5 in the present study], and finds nearly the same diffusivity and intrinsic attenuation as those determined for the two-dimensional diffusion model. The corresponding Q_S^{-1} spans the interval between 0.6 to 0.07 . The values are similar to those obtained at Merapi. At Mt. Vesuvius the diffusive layer thickness is found to be of the order of 1 km , and the results for a diffusive layer over a half-space are similar to those for a homogeneous model. This is due to the source receiver distance range used, that is always greater than the thickness of the diffusive layer. The results for Mt. Vesuvius appear to be independent of the boundary conditions used.

ENERGY TRANSPORT THEORY APPLIED TO EARTHQUAKE DATA

Uniform half space

Del Pezzo et al (2006) use earthquakes instead of shot-data to measure the scattering properties of the earth materials beneath Mt. Vesuvius. These authors use the energy transport theory in the approximation of Zeng (1991), given by

$$\begin{aligned} E_{MS}(\mathbf{x}, t, \eta_i, \eta_S) \quad &\simeq \quad E_0 e^{-(\eta_i+\eta_S)\beta t} \left[\delta \frac{(t-\frac{|\mathbf{x}|}{v})}{4\pi\beta\left|\mathbf{x}\right|^2} + \eta_s \frac{H(t-\frac{|\mathbf{x}|}{\beta})}{4\pi\beta\left|\mathbf{x}\right| t} \ln \frac{1+\frac{|\mathbf{x}|}{\beta t}}{1-\frac{|\mathbf{x}|}{\beta t}} \right] + \\ &+ cH(t-\frac{|\mathbf{x}|}{\beta})(\frac{3\eta_s}{4\pi\beta t})^{\frac{3}{2}} e^{-\frac{3\eta_s|\mathbf{x}|^2}{4\beta t}-\eta_i\beta t} \end{aligned} \tag{8}$$

where $c = E_0 \frac{\left[1-(1+\eta_s\beta t)e^{-\eta_s\beta t}\right]}{\frac{4}{\sqrt{\pi}}\int_0^{\frac{\sqrt{3\eta_s\beta t}}{2}} e^{-\alpha^2}\alpha^2 d\alpha}$; symbols are the same as for equation (3). This equation was fit to the average normalized energy coda envelope calculated for two stations, BKE and OVO of the local seismic network [see Fig. 1 of Del Pezzo et al (2006)] . These two stations are approximately 1 km distant from each other, and are located respectively eastward and westward from the crater. The assumptions of this theory are constant velocity and scattering coefficient in a uniform random medium .

This study used the stacked S-coda envelope at BKE and OVO obtained by filtering seismograms in four frequency bands, centered respectively at $f_c = 3, 6, 12$ and 18 Hz with a bandwidth of $\pm 0.3 f_c$. The stack is achieved by aligning all the three component envelopes at the P-wave onset time and normalizing to the coda level at $11s$ lapse time. The average coda is fit to the theoretical model of formula (8) starting at a lapse time of twice the S-wave travel time, after which all the envelopes have a smooth and regular time decay. A further fit of the same data was also done to the diffusion model [equation (7)].

The results are given in Figure 5. Details on the misfit function at 1σ confidence level are given in Del Pezzo et al (2006). The errors are always of the order of $\pm 25\%$ of the estimated value. From Figure 5 it appears clear that 3-component stack and vertical component average energy envelope share the same pattern and yield the same result. Multiple scattering (MS) and diffusion models (DF) furnish the same results, whereas single scattering approximation (Q_C^{-1}) gives different results. This last result indirectly indicates that the diffusion regime is also appropriate to describe the seismic energy decay in the coda at Mt. Vesuvius for natural VT earthquakes, confirming the results obtained for shot data. The most important condition for the validity of the diffusion approximation is that the lapse time, t, should be greater than the transport mean free path divided by the wave velocity:

$$t_{lapse} > L/\beta \tag{9}$$

Taking $\beta = 1.5$ km/s and estimating the mean free path L from the estimates of Q_S^{-1} obtained by Del Pezzo et al (2006) through the formula (Sato and Fehler, 1998)

$$Q_S^{-1} = \frac{\beta}{2\pi f L} \tag{10}$$

Results show that for OVO station $L \simeq 0.7$ km for frequencies centered at 3 and 6 Hz and $L > 5$ km for higher frequency; for BKE station $L \simeq 0.5$ km in the whole frequency range investigated. Since the lapse-time window utilized by Del Pezzo et al (2006) is in the range from 4 to 12 s, inequality (9) is fulfilled except for the highest frequency band at OVO.

Possible bias introduced by assuming a uniform diffusive layer

On the basis of the results obtained by a velocity tomography study carried out by Scarpa et al (2002), Del Pezzo et al (2006) assume a simplified two-layer structure for Mt. Vesuvius: the first layer with $Vp = 2.6$ km/s from the crater top down to the limestone interface overlying a half space with $Vp = 4.5$ km/s. A further assumption is that the S-wave velocity is estimated by the P-velocity divided by the Vp/Vs ratio [1.8, averaged from the values reported in Scarpa et al (2002)]. Hereafter, I will call MODEL1 the uniform half-space and MODEL2 the two-layers model.

Del Pezzo et al (2006) use the analytical solution for the diffusion equation obtained for a thick layer over a homogeneous half-space, described by Wegler (2004) assuming a) that diffusivity D (see eq. 7) is constant in the top layer of MODEL2 and b) that the whole diffusion process takes place in the same layer. They check both the cases of a fully absorbing boundary between the two layers and a fully reflecting interface [equation 16 and 18 of Wegler (2004) respectively] comparing the energy envelopes obtained for MODEL2 with those calculated for MODEL1. The results are that the coda energy envelope for MODEL1 calculated with the diffusion parameter, $D_{uniform}$, is well approximated by the energy envelopes in MODEL2 with $D_{absorbing} \simeq D_{uniform}$ and $D_{reflecting} \simeq 2D_{uniform}$. This result indicates that an earth model more realistic than the half space may introduce severe biases into estimate of diffusivity. These may be introduced by neglecting the effects of the leakage, as described in Margerin et al (1998) , whereas the diffusion constant may be not severely influenced by the simplified assumptions. The bias introduced by the simplifying assumption of half space has been demonstrated for shot data fired at Mt. Vesuvius by Wegler (2004) and has thus been confirmed also for natural seismicity. This should be taken into account for any comparisons among different volcanic zones.

Coda localization effects

Aki and Ferrazzini (2000) observed at Piton de la Furnaise volcano (PdF) that the coda site amplification depends on source position when sources are close to the crater and that most of the scattered energy is produced near the source. This phenomenon has been called coda localization. The same phenomenon was claimed to explain the energy coda shape observed at Merapi volcano by Friederich and Wegler (2005). This study showed that in their area of investigation the coda energy envelope had the same systematic decrease with increasing source-receiver distance, different from the general observation of Aki and Chouet (1975) that the coda energy tends to a common level independent of source-receiver distance. The Ioffe Regel criterion $kL < 1$ [k is the wave number and L is the scattering mean free path - Van Tiggelen (1999)] is met in their data. This is the condition for the application of the Anderson localization model (Van Tiggelen, 1999). In this scattering regime Weaver (1994) found phenomenologically a formula describing the energy density decay E as a function of distance r and lapse time t, which includes the intrinsic dissipation:

$$E(r,t) = E_0 \exp(-\frac{r}{\xi} - (\frac{r^{2+n}}{4D_{res}t\xi^n})^h - bt) \quad (11)$$

where n and h are empirically determined constants (assumed to be respectively equal to 0.46 and 0.76), ξ is the localization length, D_{res} is the residual diffusivity and b is the intrinsic dissipation coefficient. Friederich and Wegler (2005) compared the Anderson localization model with the half space diffusion model fitted to their data using both equations (11) and (7). They saw that at Merapi the energy envelopes as a function of distance and lapse time fit well to formula (11) in the frequency band between 1 and 3 Hz with $D_{res} \simeq D = 0.12km^2/s$; $b = \frac{2\pi f}{Q_I^{-1}} = 0.2s^{-1}$; $\xi = 1.7km$.The condition $kL < 1$ indicates that the Anderson localization regime may be present in their data at low frequency, with a localization length ξ . It is important to note that, however, the spatial localization of coda energy can also be explained, according to Friederich and Wegler (2005) as a result of an inhomogeneous distribution of scattering strength.

For earthquake data recorded at Mt. Vesuvius the Ioffe-Regel criterion is not met in the investigated frequency bands. Taking $v = 1.5$ km/s and estimating the mean free path L from the estimates of Q_S^{-1} obtained through the formula (10) we have for OVO station $13 < kL < 7 \cdot 10^3$ and for BKE station $6 < kL < 48$, well outside the limits given by $kL < 1$. In conclusion, the difference at OVO should be not a distance effect, as OVO and BKE are almost equally distant from the location centroid of VT earthquakes. The different energy envelope shape between OVO and BKE may be interpreted as being due to different scattering conditions between the N-Western part of Mt Vesuvius, where OVO is set up, and the Eastern part of the volcano, where most of the other seismic stations are located.

CONCLUDING REMARKS

In the present chapter I have described the results obtained from fitting several scattering models to the seismic coda envelopes of volcanic earthquakes and artificial shots fired in volcanic structures. The estimates of coda-Q values on volcanoes [made with the single scattering model] are only slightly smaller than those measured in non-volcanic zones, and the frequency dependence of coda-Q in volcanic areas is sometimes different from that in tectonically active regions. However, it is impossible to deduce using only coda-Q observations whether this difference between the coda-Q estimates in volcanic and non-volcanic zones is controlled more by intrinsic or by scattering attenuation.

In contrast, the application of multiple scattering models allows a separate estimate of the scattering and intrinsic attenuation parameters. The main results obtained in volcanoes show in general that, at low frequency, intrinsic dissipation is more important, whereas scattering predominates at high frequencies. Volcanoes are consequently heterogeneous structures with a mechanism of seismic wave energy dissipation that tends to be controlled by the scattering phenomena with increasing frequency. For Mt. Vesuvius, Mt. Merapi and Deception Island volcano scattering attenuation prevails at frequencies higher than 2-3 Hz, but unfortunately there is no informations for lower frequencies. At Mt. Etna intrinsic dissipation prevails or is comparable with scattering attenuation for frequencies lower than 8 Hz. This result, obtained in the early 1990's with the use of approximate models, has been confirmed by the application of the energy transport theory to both earthquakes and tremor. At a first sight, it sounds unexpected, as one can image volcanoes as structures where the magma reservoirs, partially filled with melted, high temperature rocks, intrinsically dissipate the seismic energy. This seems to happen only at low frequency. The difference in the pattern of attenuation between low- and high-frequencies can be explained in terms of the scale length of heterogeneity. Volcanoes may represent non self-similar earth medium, characterized by one or more predominant characteristic correlation length.

As a consequence of the high degree of heterogeneity in volcanoes, the seismograms of VT events can visually appear different in shape from the corresponding magnitude seismograms of non-volcanic earthquakes. In fact, the coda of volcanic earthquakes is longer than that for earthquakes generated with the same magnitude in less heterogeneous environments, including tectonically active non-volcanic areas. Moreover, the maximum of the energy envelope for volcano earthquakes (VT) is more delayed with respect to the time of S-onset than that for non-volcanic earthquakes.

Unfortunately, a comparison among the investigated volcanoes is only partial, as seismograms from both shots and VT earthquakes recorded at Mt. Vesuvius have a sufficient signal to noise ratio only at high frequency, in contrast to those of Etna and Merapi. Consequently, the best estimate of separated intrinsic- and scattering-attenuation is stable for Mt. Vesuvius only at high frequencies and we have no information in the low frequency band between 1 and 5-6 Hz. Further efforts need be made towards quantifying the observation at low frequencies on this volcano and in general on different volcanoes, to determine if the difference in the attenuation pattern at low and high frequencies could be ascribed to a general phenomenon, peculiar for volcanic environments, or to the geological characteristics of only some volcanoes.

Quantification of the scattering properties is seen also to be very useful in the physical interpretation of the seismic phenomena accompanying volcanic eruptions. Recent results have shown that small changes in the elastic properties of the medium, that have no detectable influence on the first arrivals, are instead amplified by multiple scattering and may thus be readily observed in the coda. This idea is quantified in the concept of coda wave interferometry (see another chapter of this book) that is going to be one of the most promising techniques to monitor the temporal changes of the scattering coefficients of the earth medium [see Gret et al (2005) and references therein]. So, knowledge of the average scattering properties may help in quantifying the effects on the earth medium of the stress changes acting on volcanoes before and during the eruptive periods. This knowledge is also very useful in the interpretation of the attenuation tomographic images obtained in volcanoes. Recent work by Nishigami (1997) and Tramelli et al (2006) among others, show that most of the strong scattering in volcanoes takes place in zones with maximum contrast in their geological characteristics. Tramelli et al (2006) show, for example, that the border between the old caldera rim and the central new caldera zone at Campi Flegrei is characterized by the maximum positive spatial change in the scattering coefficient. As this zone coincides with that of maximum total attenuation, this is an indirect confirmation that the low-total Q zones in volcanoes are often associated with low scattering-Q.

References

Abubakirov, I.R. and Gusev, A.A. (1990) Estimation of scattering properties of the lithosphere of Kamchatka based on Monte Carlo simulation of record envelope of near earthquake. Phys. Earth and Pl. Int. 64, 52-67

Aki, k. and B. Chouet (1975). Origin of coda waves: source, attenuation and scattering effects, J. Geophys. Res 80, 3322-3342.

Aki, K. and Ferrazzini, V. (2000). Seismic monitoring and modeling of an active volcano for prediction, J. Geophys. Res., 105 (B7) 16617-16640.

Baiji, Li Jiazheng, Qin Jianqing Ye Mingong Chen Xuejun Liu (2000) Primary Study On Attenuation Of Shear Wave And Coda In Tengchong Volcano Areas Journal of Seismological Research (China) Vol.23 No.2

Benz, H.M., Chouet, B., Dawson, P.B., Lahr, J.C., Page, R.A., Hole J.A. (1996) Three dimensional P and S velocity structure of Redoubt Volcano, Alaska. J.Geophys. Res., 99, 8111-8128

Bianco, F., Del Pezzo, E., Castellano, M., Ibanez, J.M., Di Luccio, F. (2002) Separation of Intrinsic and scattering Seismic Attenuation in the Southern Apennine zone, Italy. Geophys. J. Int. 150: 10-22.

Bianco, F., Castellano, M., Del Pezzo, E. and Ibanez, J.(1999) Attenuation of the short period seismic waves at Mt. Vesuvius, Italy. Geophys. J. Int. Volume 138, Issue 1, July 1999 pp 67-76

Bianco, F., Cusano, P., Petrosino, S., Castellano, M:, Buonocunto, C., Capello, M., and Del Pezzo, E. (2005) Small-aperture array for seismic monitoring of Mt. Vesuvius. Seismological research Letters, 76, 344-355.

Canas, J.A., Pujades, L.G., Blanco, M.J., Soler, V., Carracedo, J.C. (1995) Coda-Q distribution in the Canary Islands. Tectonophysics, 246, 245-261

Castellano, M., Buonocunto, C., Capello, M. and La Rocca, M. (2001) Seismic surveillance of active volcanoes:the osservatorio Vesuviano Seismic Network (OVSN-Southern Italy) Seim. Res. Letters, 73,2

Chouet, B., 2003. Volcano seismology. Pure and applied geophysics, 160 739-788.

Del Pezzo, E., Lombardo, G. and Spampinato,S. (1989). Attenuation of volcanic tremor at Mt Etna, Sicily. Bull.Seism.Soc .Am, 79,6, 1989-1994.

Del Pezzo, E., Ibanez, J., Morales, J., Akinci, A., Maresca, R. (1995) Measurements of intrinsic and scattering attenuation in the crust. Bull. Seism. Soc. Am., 5, 1373-1380.

Del Pezzo, E., Simini, M., Ibanez, J.M., 1996. Separation of intrinsic and scattering Q for volcanic areas: a comparison between Etna and Campi Flegrei. J. Volcanol. Geoth. Res., 70, 213-219.

Del Pezzo, E., Bianco, F., Saccorotti, G. (2001) Separation of intrinsic and scattering Q for volcanic tremor: an application to Etna and Masaya Volcanoes. Geophys. Res. Letters, 28, 3083-3086

Del Pezzo, E., Bianco, F. and Zaccarelli, L. Separation of Qi and Qs from passive data at Mt. Vesuvius: a reappraisal of seismic attenuation. Physics of the Earth and Planetary Interiors, 159, 202-212.

Frankel, A. and Clayton, R.W., (1986) Finite difference simulations of seismic scattering Implications for the propagation of short-period seismic waves in the crust and models of crustal heterogeneity. J. Geophys. Res., 91,6465-6489.

Frankel, A., and Wennerberg, L. (1987). Energy Flux model of seismic coda - separation of scattering and intrinsic attenuation. Bull. Seism. soc. Am., 77, 1223-1251.

Friederich, C. and Wegler, U. (2005) Localization of the seismic coda at Merapi volcano (Indonesia). Geophys. Res. Letters, 32, L14312 doi:101029.

Gasparini, P. and TOMOVES Working group, 1998. Looking inside Mt. Vesuvius. Eos, 79 (19) 229-232.

Gret, A., R. Snieder, R. C. Aster, and P. R. Kyle (2005). Monitoring rapid temporal change in a volcano with coda wave interferometry, Geophys. Res. Lett., 32, L06304,doi:10.1029/2004GL021143.

Gusev, A. A. (1995). Vertical profile of turbidity and coda Q. Geophysical Journal International 123, 3, 665-672.

Gusev, A. A. and Abubakirov, I. R. (1996) Simulated envelopes of non isotropically scattered body waves as compared to observed ones : another manifestation of fractal heterogeneity Geophysical journal international, 127, pp. 49-60.

Hoshiba, M., 1991. Simulation of multiple-scattered coda wave excitation based on the energy conservation law. Physics of the Earth and Planetary Interiors 67, 123-136, doi = {10.1016/0031-9201(91)90066-Q}

Hoshiba, M., Sato, H., Fehler, M., 1991. Numerical basis of the separation of scattering and Intrinsic absorption from full seismogram envelope - a Montecarlo simulation of multiple Isotropic scattering. Papers in meteorology and Geophysics, 42, 2, 65-91.

Hoshiba, M., Rietbrock, A., Scherbaum, F., Nakahara H. and Haberland, C. (2001). Scattering attenuation and intrinsic absorption using uniform and depth dependent model – Application to full seismogram envelope recorded in Northern Chile. Journal of Seismology, 5, 157-179, DOI 10.1023/A:1011478202750.

Hoshiba, M. (1993). Separation of scattering attenuation and intrinsic absorption in Japan using the multiple lapse time window analysis of full seismogram envelope. J Geophys. Res., 98, B9, 15809-15824.

Ibanez, J.M., 1990. Atenuacion de ondas coda y Lg en el sur de Espana y de Italia a partir de sismogramas digitales. Tesis Doctoral, Universidad de Granada. pp. 306.

Jin, A., Mayeda, K., Adams, D., Aki, K. (1994). Separation of intrinsic and scattering attenuation in Southern California using TERRAscope data. J.Geophys.Res. 99, 17835-17848.

La Rocca, M., Del Pezzo, E., Simini, M., Scarpa, R., De Luca, G. (2001) Array analysis of seismograms from explosive sources: evidence for surface waves scattered at the main topographical features. Bull. Seism. Soc. Am. 91,2 219-231

Lomax, A., J. Virieux, P. Volant and C. Berge, (2000). Introduction of a Metropolis-Gibbs method and comparison with linear locations. In Advances in Seismic Event Location, C. Thurber, E. Kissling, N. Rabinowitz (eds.) Kluwer, Amsterdam.

Mayeda, K., Koyanagi, S. and Aki, K. (1992) A comparative study of scattering, intrinsic and coda Q^{-1} for Hawaii, Long Valley and Central California between 1.5 and 15.0 Hz J.Geophys. Res., 97,6643-6659

Margerin, L., Campillo, M. and Bart van Tiggelen, 1998. Radiative transfer and diffusion of waves in a layered medium: new insight into coda Q Geophys. J. Int. 134, 596 - 612.

Martinez Arevalo, C., Bianco, F., Ibanez, J., Del Pezzo , E. (2003) Shallow seismic attenuation and shear wave splitting in the short period range of Deception Island volcano (Antarctica). J. Volcanol. Geoth. Res., 128, 1-3, 89-113.

Matsunami, K., 1991. Laboratory tests of excitation and attenuation of coda waves using 2-D models of scattering media.Physics of the Earth and Planetary Interiors, 67, 36-47 doi = {10.1016/0031-9201(91)90058-P}

Matsunami, K., Nakamura, M. 2004 Seismic attenuation in a non volcanic swarm region beneath Wakayama, southwest Japan. J. Geophys. Res, 109, B09302, doi:10.129/2003JB002758

Metaxian, J.P., Lesage, P., Dorel, J., 1997. Permanent tremor of Masaya volcano, Nicaragua: Wavefield analysis and source location. J. Geophys. Res., 102, 22529-22545,

Nishigami, K. (1997) Spatial distribution of coda scatterers in the crust around two active volcanoes and one active fault system in central Japan: inversion analysis of the coda envelope Physics of the Earth and Pl. Int., 104, 75-89.

Ryzhik, L.V., G.C. Papanicolaou and J.B. Keller, (1996) Transport equation for elastic and other waves in random media, Wave Motion 24, 327-370.

Sato, H. (1993). Energy transportation in one- and two-dimensional scattering media : analytic solutions of the multiple isotropic scattering model. Geophysical J. Int., 112, no1, pp. 141-146.

Sato, H. and Fehler, M. C. (1998) Seismic wave propagation and scattering in the heterogeneous earth.Springer-Verlag, New York

Scarpa R., Tronca F., Bianco F., Del Pezzo E., 2002. High resolution velocity structure beneath Mount Vesuvius from seismic array. Geophys. Res. Let., 29 (21), 2040.

Shang, T. and Gao, L (1988). Transportation theory of multiple scattering and its application to seismic coda waves of impulsive source. Scientia Sinica (series B, China) 31, 1503–1514

Tramelli, A., Del Pezzo, E. Bianco, F. and Boschi, E., 2006. 3-D scattering image of the Campi Flegrei caldera (Southern Italy). New hints on the position of the old caldera rim. Physics of the Earth and Planetary Interiors. 155, 269-280

Van Tiggelen, B.A., 1999. Localization of waves, in Diffuse waves in complex media, edited by J.P. Fouque, Kluwer Academic Publisher, Dortrecht, The Netherlands 1, 60

Weaver, R.L., 1994. Anderson localization in time domain: numerical studies of waves in two dimensional disordered media, Phys. Rev. B, 49(9), 5881-5895

Wegler, U. and Luhr, B.G. (2001) Scattering behaviour at Merapi Volcano, Java revealed from an active seismic experiment Geophys. J. Int., 145, 579-592

Wegler, U. (2003) Analysis of multiple scattering at Vesuvius volcano, Italy, using data of the TomoVes active experiment. Journal Volcanol. Geoth. Res., 128, 45-63.

Wegler, U. (2004) Diffusion of seismic waves in a thick layer: Theory and application to Vesuvius volcano (2004). J. Geophys. Res. 109, B07303, doi:10.1029/2004JB003048

Wegler, U. (2005) Diffusion of seimic waves in layered media: boundary conditions and analytical solutions. Geophys. J. Int., 163, 1123-1135.

Wennerberg, L. (1993) Multiple scattering interpretation of coda-Q measurements. Bull. Seism. Soc. Am. 83, 279-290

Wong, W., Rebollar, C.J., Munguia, L. (2001) Attenuation of Coda Waves at the tres Virgenes Volcanic Area, Baja California Sur, Mexico. Bull. Seism. Soc. Am., 91, 683-693.

Wu, R.S. (1985) Multiple scattering and energy transfer of seismic waves - separation of scattering effects from intrinsic attenuation - I. Theoretical modeling, Geophys. J. R. Astron. Soc. 82, 57-80.

Zeng, Y., 1991. Compact solutions for multiple scattered wave energy in time domain. Bull., Seimol., Soc., Am. 81, 1022-1029.

FIGURE CAPTIONS

Figure 1.Q_C^{-1} as a function of frequency, calculated for several volcanic areas around the world. References are: Campi Flegrei (Bianco et al, 1999) ; Etna (Del Pezzo et al, 1996) ; Deception (Martinez Arevalo et al, 2003); Tres Virgenes (Wong et al, 2001) ; Tengchong (Baiji et al, 2000); Canary Islands Canas et al (1995); KilaueaMayeda et al (1992); Mt S. Helens (Bianco et al, 1999). Lapse time intervals in which the fit to the single scattering model has been carried out are also given. Data from the literature with no explicit report of lapse time interval have been disregarded.

Figure 2. Comparison of Q_C^{-1} vs frequency, calculated for the same lapse time interval at Etna volcano and in Andalucia (Granada basin- Southern Spain). Despite the similar frequency patterns the values of attenuation are different; higher for Etna volcano than for the tectonically active region of Andalucia.

Figure 3. Q_I^{-1} and Q_S^{-1} obtained using the approximate method of Wennerberg for Etna volcano, Deception Island volcano and Andalucia.

Figure 4. Diffusion model under the assumption of a half space applied to shot data recorded at Merapi and Mt. Vesuvius. The patterns of both Q_I^{-1} and Q_S^{-1} are similar for the two volcanoes. Scattering attenuation prevails over the intrinsic dissipation of about one order of magnitude.

Figure 5. a) Left panel shows Q_C^{-1}, Q_I^{-1}, Q_S^{-1}, Q_T^{-1} ($= Q_I^{-1} + Q_S^{-1}$) for BKE station- three component stack (see Del Pezzo et al (2006) for the station location); The right panel shows the same quantities for BKE vertical

Q_S^{-1}			n
6 Hz	8 Hz	10 Hz	
0.004 ± 0.001	0.005 ± 0.001	0.005 ± 0.001	0.1
0.05 ± 0.01	0.04 ± 0.01	0.031 ± 0.007	0.9
Q_I^{-1}			
6 Hz	8 Hz	10 Hz	
0.00365 ± 0.00007	0.0031 ± 0.0001	0.0028 ± 0.0001	0.1
0.00357 ± 0.00006	0.0031 ± 0.0001	0.0027 ± 0.0001	0.9

Table 1. Separation of inverse Qi and Qs for Campi Flegrei. Values are re calculated from Table 2 of Del Pezzo et al. (1996)

Volcano	Frequency(Hz)	Q_I^{-1}	$\sigma_{Q_I^{-1}}$	Q_S^{-1}	$\sigma_{Q_S^{-1}}$
Etna	1	0.2	0.4	0.009	0.005
	2	0.5	2	0.005	0.001
	3	1	10	0.010	0.001
	4	0.3	7	0.009	0.007
	5	0.1	0.2	0.005	0.002
Masaya	2	0.2	0.5	0.04	0.02
	3	0.1	0.5	0.005	> 0.001

Table 2. Separation of inverse Qi and Qs for volcanic tremor at Etna and Masaya. Values are re calculated from Table 1 of Del Pezzo et al. (2001)

component only. b) The same of for OVO station. 3D Q_C^{-1} and 2D Q_C^{-1} values were obtained using different geometrical spreading (body waves and surface waves respectively).

ACKNOWLEDGEMENT

This work is financed by INGV-DPC projects V3_4 and V4, MIUR-FIRB project entitled "Analisi del campo d'onda associato al vulcanismo attivo" and EU project "VOLUME". Francesca Bianco, Anna Tramelli and Luca De Siena are gratefully acknowledged for their suggestions. Mike Fehler and two anonimous reviewers greatly helped in improving the manuscript. Chris Berrie corrected the English style.

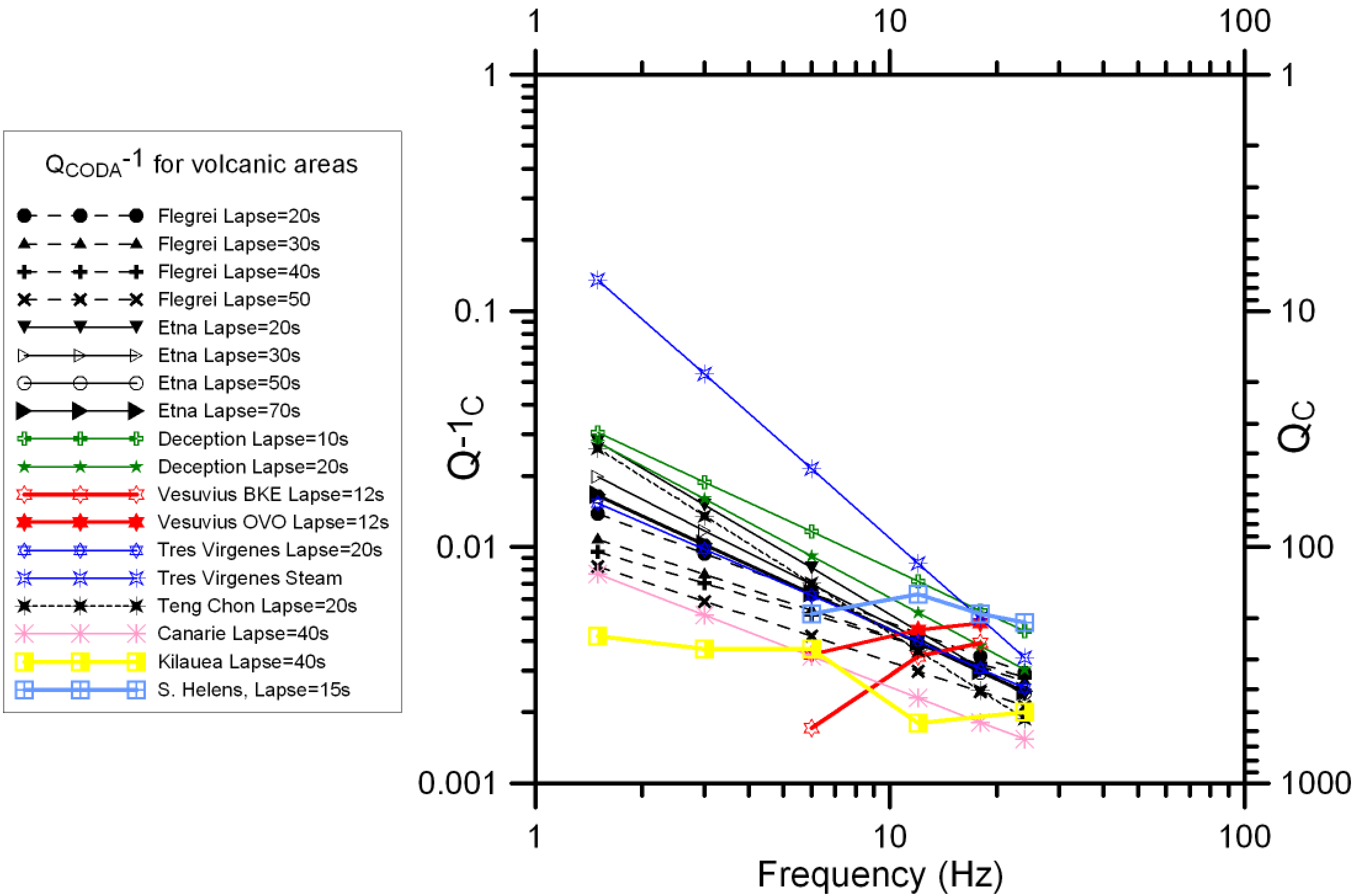

Q$_{CODA}^{-1}$ for volcanic areas
Flegrei Lapse=20s
Flegrei Lapse=30s
Flegrei Lapse=40s
Flegrei Lapse=50
Etna Lapse=20s
Etna Lapse=30s
Etna Lapse=50s
Etna Lapse=70s
Deception Lapse=10s
Deception Lapse=20s
Vesuvius BKE Lapse=12s
Vesuvius OVO Lapse=12s
Tres Virgenes Lapse=20s
Tres Virgenes Steam
Teng Chon Lapse=20s
Canarie Lapse=40s
Kilauea Lapse=40s
S. Helens, Lapse=15s
Q^{-1}_C
Q_C
Frequency (Hz)
1
10
100
0.001
0.01
0.1
1
10
100
1000

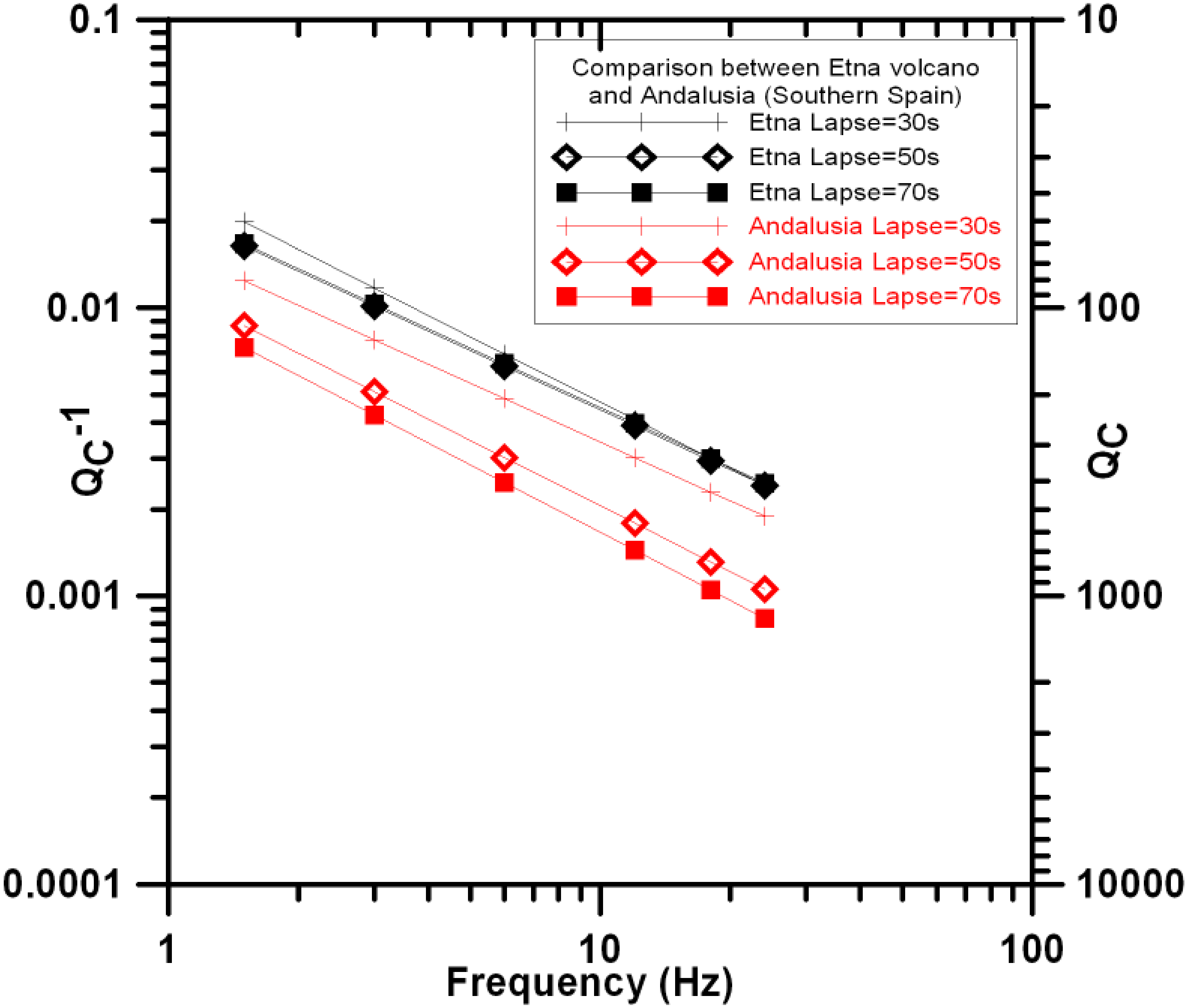

Comparison between Etna volcano
and Andalusia (Southern Spain)
Etna Lapse=30s
Etna Lapse=50s
Etna Lapse=70s
Andalusia Lapse=30s
Andalusia Lapse=50s
Andalusia Lapse=70s
Q_C^{-1}
Q_C
Frequency (Hz)
0.1
0.01
0.001
0.0001
10
100
1000
10000
1
10
100

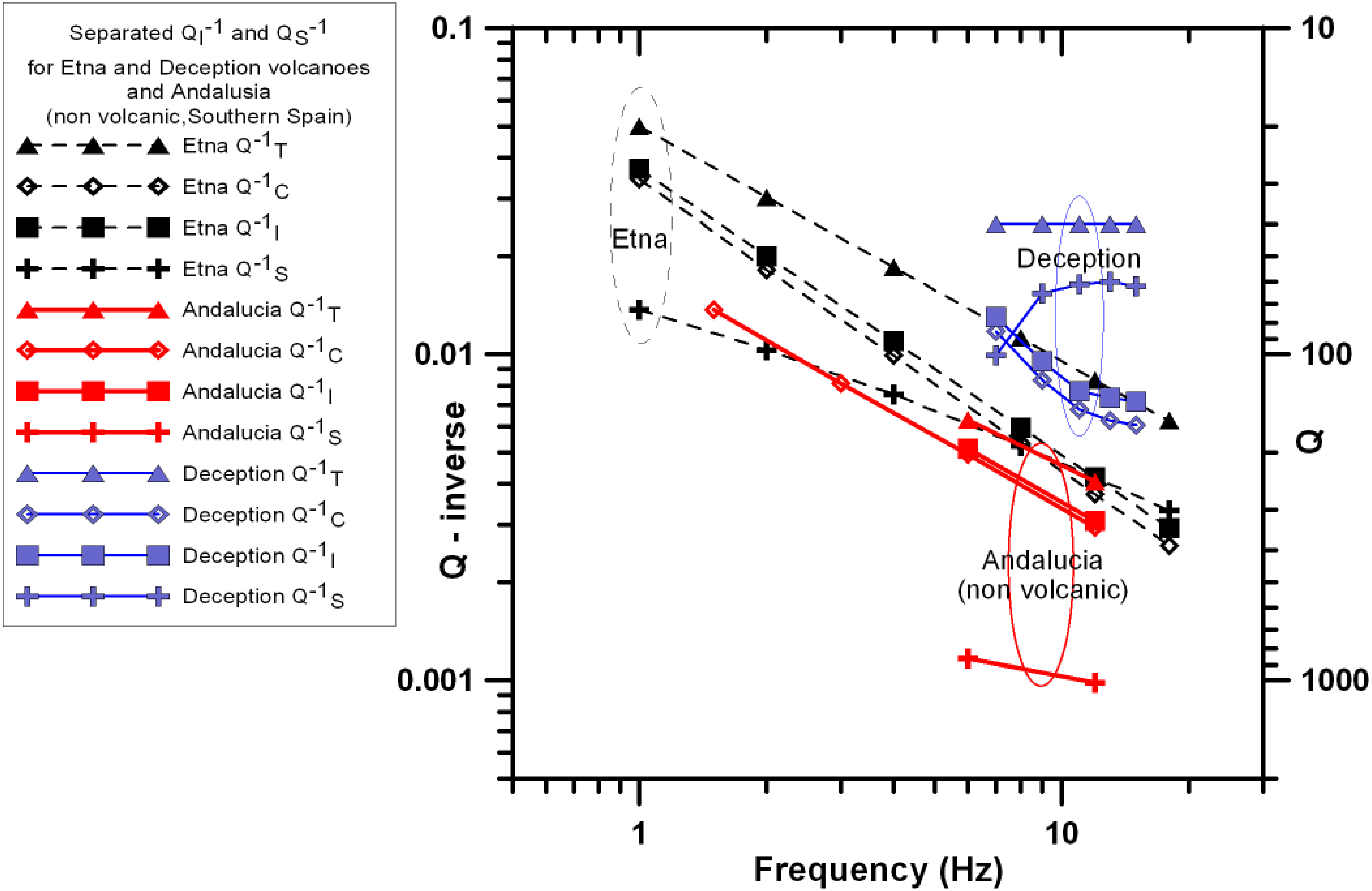

Separated Q_I^{-1} and Q_S^{-1}
for Etna and Deception volcanoes
and Andalusia
(non volcanic,Southern Spain)
Etna $Q^{-1}{}_T$
Etna $Q^{-1}{}_C$
Etna $Q^{-1}{}_I$
Etna $Q^{-1}{}_S$
Andalucia $Q^{-1}{}_T$
Andalucia $Q^{-1}{}_C$
Andalucia $Q^{-1}{}_I$
Andalucia $Q^{-1}{}_S$
Deception $Q^{-1}{}_T$
Deception $Q^{-1}{}_C$
Deception $Q^{-1}{}_I$
Deception $Q^{-1}{}_S$
0.1
0.01
0.001
10
100
1000
Q - inverse
Q
Etna
Deception
Andalucia
(non volcanic)
1
10
Frequency (Hz)

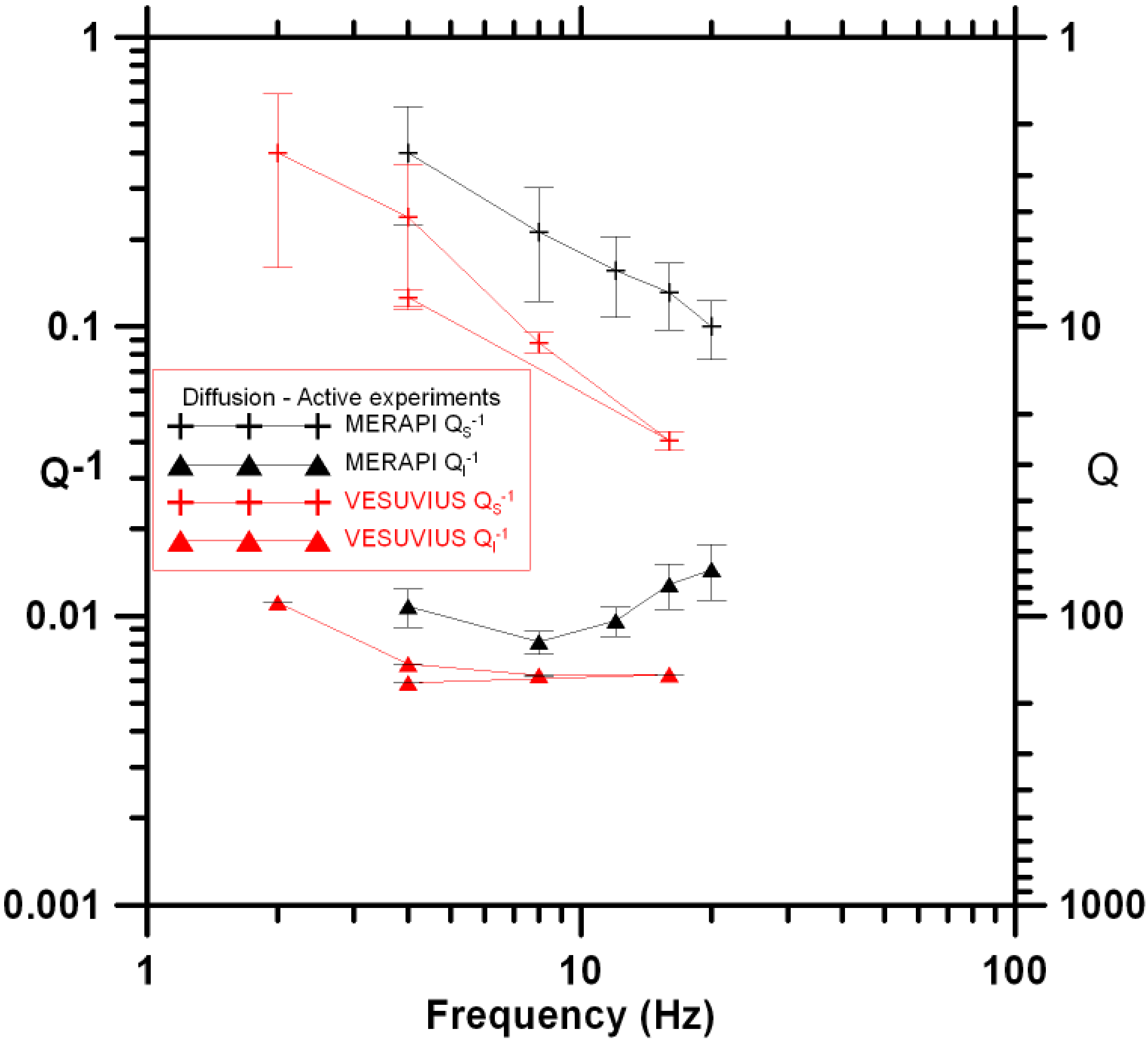

1
0.1
0.01
0.001
Q-1
1
10
100
1000
Q
1
10
100
Frequency (Hz)
Diffusion - Active experiments
MERAPI Q_S^{-1}
MERAPI Q_I^{-1}
VESUVIUS Q_S^{-1}
VESUVIUS Q_I^{-1}

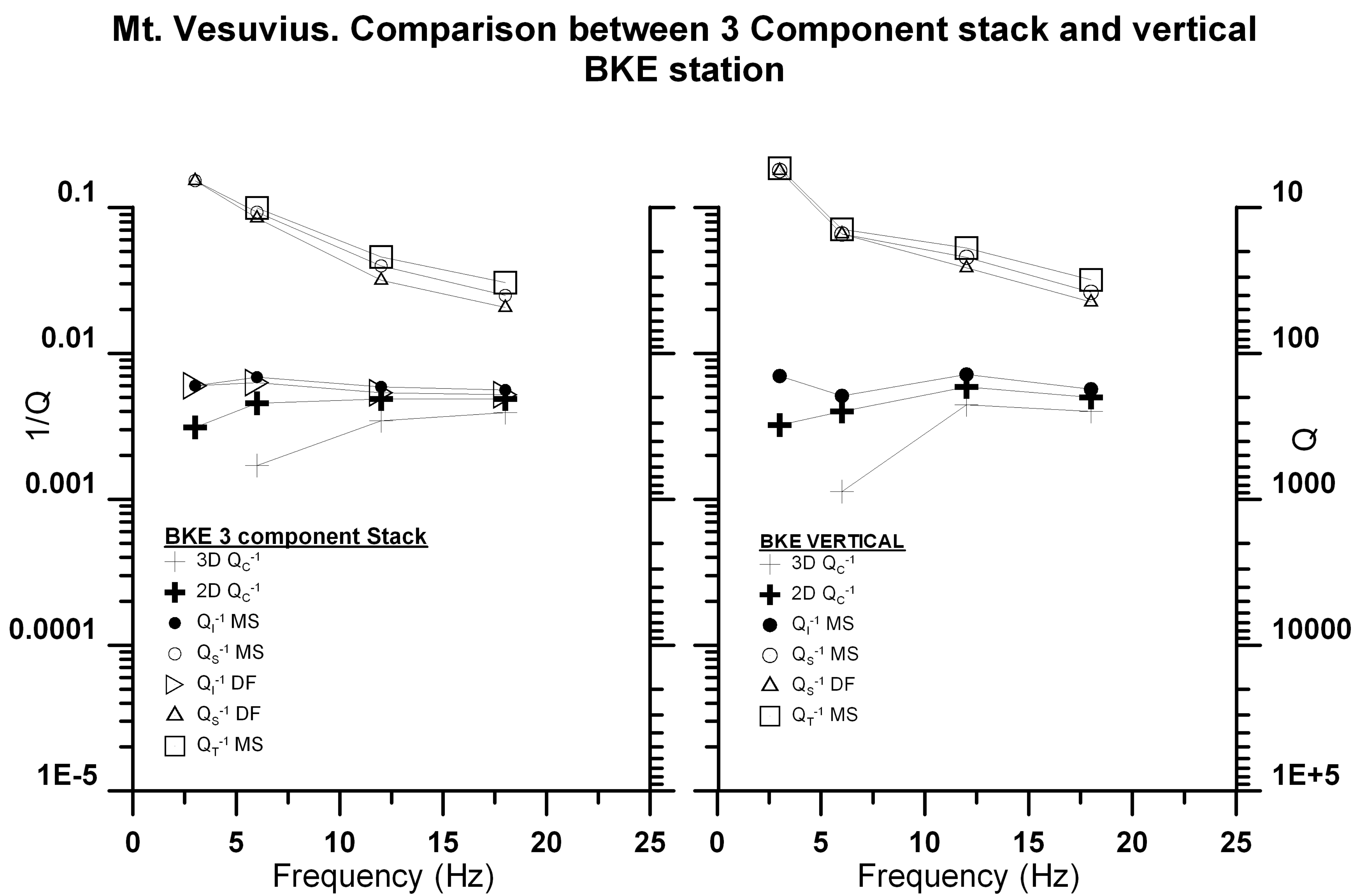
Mt. Vesuvius. Comparison between 3 Component stack and vertical
BKE station
1/Q
Q
0.1
0.01
0.001
0.0001
1E-5
10
100
1000
10000
1E+5
0
5
10
15
20
25
Frequency (Hz)
BKE 3 component Stack
3D Q_C^{-1}
2D Q_C^{-1}
Q_I^{-1} MS
Q_S^{-1} MS
Q_I^{-1} DF
Q_S^{-1} DF
Q_T^{-1} MS
BKE VERTICAL
3D Q_C^{-1}
2D Q_C^{-1}
Q_I^{-1} MS
Q_S^{-1} MS
Q_S^{-1} DF
Q_T^{-1} MS

Mt. Vesuvius. Comparison between 3 component stack and Vertical OVO station